Toppan Best-set Premedia Limited
Journal Code: EMI4 | Proofreader: Mony
Article No: EMI412015 | Delivery date: 23 Nov 2012
Page Extent: 9
EMI412015

Environmental Microbiology Reports (2012) doi:10.1111/1758-2229.12015

Distinct lipopeptide production systems for WLIP (white line-inducing principle) in *Pseudomonas fluorescens* and *Pseudomonas putida*

Hassan Rokni-Zadeh, Wen Li, Eshetu Yilma,† Aminael Sanchez-Rodriguez and René De Mot*
Centre of Microbial and Plant Genetics, KU Leuven, Kasteelpark Arenberg 20, B-3001 Heverlee-Leuven, Belgium.

Summary

The interaction of WLIP (white line-inducing principle), a member of the viscosin group of *Pseudomonas* lipopeptides, with tolaasin, a lipopeptide mycotoxin secreted by *Pseudomonas tolaasii*, enables identification of the mushroom pathogen relying on formation of a lipopeptide coprecipitate between confronted colonies of an indicator strain (designated *Pseudomonas 'reactans'*) and *P. tolaasii*. The WLIP non-ribosomal lipopeptide synthesis system of the mushroom isolate *P. 'reactans'* LMG 5329 (Wip) was identified and shown to be most similar to the *Pseudomonas fluorescens* SBW25 viscosin system (Visc), but remarkably different from the WLIP-generating Wlp system previously identified in the rice rhizosphere isolate *Pseudomonas putida* RW10S2. The Wlp machinery is composed of modules most similar to those recruited for biosynthesis of the non-viscosin-type lipopeptides putisolvin and entolysin by strains from the *P. putida* clade. In line with the pronounced synteny between the *wip* and *visc* flanking regions, strain LMG 5329 was identified as an authentic *P. fluorescens* closely related to strain SBW25. In both *P. putida* and *P. fluorescens*, WLIP production confers similar phenotypes of microbial antagonism and surface colonization. Genotypes other than *wlp* or *wip* were not identified among WLIP producers isolated from mushroom, maize rhizosphere or water.

Received 13 September, 2012; revised 29 October, 2012; accepted 2 November, 2012. *For correspondence. E-mail rene.demot@biw.kuleuven.be; Tel. (+32) 16 32 9681; Fax (+32) 16 32 1963. †Current address: School of Plant Sciences, College of Agriculture and Environmental Sciences, Haramaya University, P.O. Box 20, Dire-Dawa, Ethiopia.

© 2012 Society for Applied Microbiology and Blackwell Publishing Ltd

Introduction

Genome analyses of *Pseudomonas* strains have provided further insight into the metabolic versatility enabling their adaptation to very diverse environments (Silby *et al*., 2011; Wu *et al*., 2011; Loper *et al*., 2012). Many soil-dwelling and plant-associated isolates of these γ-proteobacteria devote a considerable part of their genome to non-ribosomal peptide synthetase (NRPS) systems that specifically activate and condense amino acids to synthesize diverse lipopeptides (Gross and Loper, 2009). Several of these amphipathic secondary metabolites have been implicated in different aspects of their producers' lifestyles, such as phytopathogenicity, microbial and predator antagonism, surface motility and biofilm formation (Raaijmakers *et al*., 2010).

Mainly based on the number (ranging from 8 to 25) and sequence of amino acids, *Pseudomonas* lipopeptides are divided into different groups (Raaijmakers *et al*., 2006; Gross and Loper, 2009; Roongsawang *et al*., 2011). A major group of *Pseudomonas* lipopeptides is constituted by the viscosin-related nonapeptides for which six subtypes have been identified: viscosin, massetolide, viscosinamide, pseudodesmin, pseudophomin and WLIP (white line-inducing principle). Within this group, a minor difference in amino acid sequence suffices to confer different biological properties. For instance, a WLIP producer induces a white line reaction (WLR) in agar medium when grown nearby a colony of the mushroom pathogen *Pseudomonas tolaasii*, because of formation of a visible co-precipitate of WLIP with the lipopeptide tolaasin (Wong and Preece, 1979). Such WLR appears to be quite structure-specific as it cannot be triggered by *Pseudomonas* strains producing lipopeptides from other groups and is even not elicited by WLIP analogues with minor structural differences, such as viscosin (fifth amino acid residue L-Leu instead of D-Leu) or viscosinamide (viscosin variant with D-Gln instead of D-Glu at position 2) (Rokni-Zadeh *et al*., 2011). For strains equipped with the capacity to produce WLIP, as used in the diagnostic test to identify tolaasin producers (Wong and Preece, 1979), the taxonomically invalid species name *Pseudomonas 'reactans'* was coined. For WLIP isolated from *P. 'reactans'* NCPPB1311 moderate antifungal activity and inhibition of Gram-positive bacteria were previously reported (Lo

UNCORRECTED PROOF

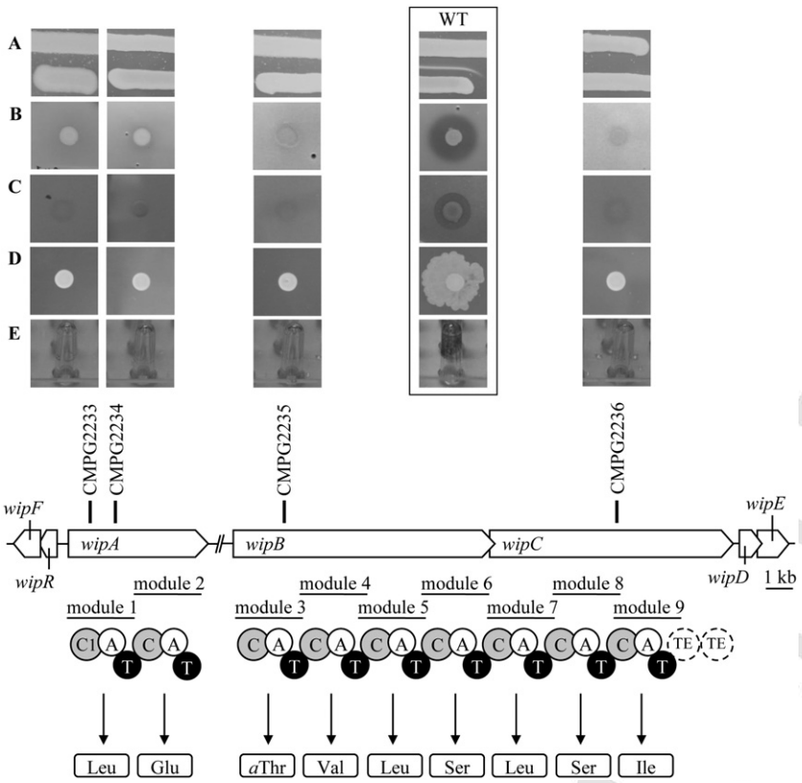

Fig. 1. Organization of the WLIP biosynthetic genes and WLIP-dependent phenotypes of *P. 'reactans'* LMG 5329. The predicted NRPS domains of WipA, WipB and WipC (labelled circles) are indicated: C, condensation; A, adenylation; T, thiolation; TE, thioesterase. C1 represents the condensation domain of the initiatory module. The amino acid specificity of the modules inferred from A-domain analysis (NRPSpredictor2; Röttig *et al.*, 2011) is shown. Transposon insertion sites in NRPS mutants lacking WLIP production are marked with vertical bars. Mutant phenotypes are compared with those of the wild type (WT): (A) WLR upon confrontation with *P. tolaasii* CH36 (upper bacterial streak), (B) antagonism against *Xanthomonas citri* pv. *malvacearum* LMG 761 (growth-inhibitory halo formation by spotted LMG 5329 cells in a *Xanthomonas* overlay), (C) haemolysis (halo formation in blood agar plates), (D) swarming on 0.8% tryptic soy agar and (E) biofilm formation on polystyrene pegs visualized by staining of adherent cells (corresponding quantitative data in the text). By homology to other similarly organized lipopeptide-associated genes in *Pseudomonas* (Rokni-Zadeh *et al.*, 2012), the linked *wipR* and *wipD-wipE-wipF* genes are predicted to encode a cognate LuxR-type regulator and a tripartite efflux transporter (composed of MacA, MacB and OprM homologues) respectively.

Cantore *et al.*, 2006). Recently, characterization of the WLIP-synthesizing NRPS system of the rice rhizosphere isolate RW10S2, belonging to the *Pseudomonas putida* cluster, further revealed a role for WLIP in antagonism of some other plant-associated γ-proteobacteria, in solid-surface translocation and in biofilm formation by its producer (Rokni-Zadeh *et al.*, 2012).

Here we report on a remarkable divergence within WLIP biosynthesis revealed upon characterization of the WLIP genetic backbone in another WLR indicator, *P. 'reactans'* LMG 5329 (Munsch and Alatossava, 2002; Sajben *et al.*, 2011) and its comparison with the other known viscosin-group NRPS systems of *Pseudomonas fluorescens* SBW25, producing viscosin (de Bruijn *et al.*, 2007), and of *P. fluorescens* SS101, producing massetolide (de Bruijn *et al.*, 2008).

Results and discussion

Identification of WLIP biosynthetic genes in P. 'reactans' *LMG 5329*

Random mutagenesis of strain LMG 5329 was carried out with the Tn*5*-delivering suicide vector pLG221 (Boulnois *et al.*, 1985). Kanamycin-resistant mutants were screened for a lack of WLR against *P. tolaasii* CH36 (Rokni-Zadeh *et al.*, 2012). For seven WLR-negative mutants, single genomic insertion of Tn*5* was confirmed by Southern hybridization (data not shown). Cloning of the DNA flanking the insertion sites by inverse PCR (Martin and Mohn, 2002) was achieved for four of these mutants and subsequent sequence analysis enabled identification of the inactivated genes in a draft genome sequence of strain LMG 5329. This was obtained by subjecting its genomic DNA, isolated using the Gentra Puregene Yeast/Bact. Kit (Qiagen), to 100-cycle pair-end sequencing with an Illumina HiSeq 2000 (Genomics Core Facility, KU Leuven). Assembly through Velvet (Zerbino and Birney, 2008) yielded 293 contigs (total size ~6.7 Mb) that were annotated automatically using RAST (Aziz *et al.*, 2008). For the contigs containing the genes disrupted in the mutants, annotations were verified by FramePlot protein-coding prediction (Ishikawa and Hotta, 1999), BLAST homology searches and Pfam domain analysis.

Analysis of the WLR-minus transposon mutants (CMPG2233-CMPG2236) enabled to locate the *wip* (WLIP production) genes (*wipA* and tandemly organized *wipB*-w*ipC*) of strain LMG 5329, encoding its three WLIP-biosynthetic NRPSs, in two unlinked genomic regions [Fig. 1; GenBank accession numbers JQ974025 (*wipA*) and JQ974026 (*wipBC*)]. Assuming consecutive co-linear biosynthesis by WipA, WipB and WipC, the predicted lipopeptide product matches the nonapeptide sequence of WLIP. The phenotypes associated with WLIP

UNCORRECTED PROOF

production in *P. putida* RW10S2, namely anti-*Xanthomonas* activity, haemolysis, swarming and biofilm formation (Rokni-Zadeh *et al*., 2012), were also identified for strain LMG 5329 wild type and found to be abolished in the LMG 5329 mutants with disrupted WLIP-biosynthetic genes (Fig. 1). Biofilm formation capacity of strain LMG 5329 on a polystyrene surface, quantified as described previously (Rokni-Zadeh *et al*., 2012), was comparable with the one of *P. putida* RW10S2. This capacity was strongly reduced in the LMG 5329 NRPS mutants: CMPG2233 (10.09 ± 0.04), CMPG2234 (9.17 ± 0.03), CMPG2235 (11.21 ± 0.03) and CMPG2236 (9.27 ± 0.05), with values in percentage relative to the wild type (set to 100%). This residual biofilm formation of on average 10% is similar to the ~10-fold reduction observed for *P. putida* RW10S2 upon inactivation of its WLIP production (Rokni-Zadeh *et al*., 2012).

The modular structure and gene organization of *wipA* (with upstream divergent *wipR*-*wipF* genes) and of unlinked *wipB*-*wipC* (with downstream convergent *wipD*-*wipE* pair) are quite similar to those reported for the NRPS gene clusters of viscosin (*P. fluorescens* SBW25 *visc* genes; de Bruijn *et al*., 2007), massetolide (*P. fluorescens* SS101 *mass* genes; de Bruijn *et al*., 2008) and WLIP (*P. putida* RW10S2 *wlp* genes; Rokni-Zadeh *et al*., 2012). The relative positions of the respective WLIP biosynthetic clusters could not be determined in the draft genomes of strains LMG 5329 and RW10S2. The similarly organized clusters for viscosin and massetolide production are separated by ~1.6 Mb in strain SBW25 (Silby *et al*., 2009) and by ~1.4 Mb in strain SS101 (Loper *et al*., 2012).

The Wip NRPSs are very similar to the Visc enzymes (~90% amino acid identity) and the Mass enzymes (82–84% amino acid identity) (Table S1). Such level of homology might be expected for these enzymes with only minor differences in catalytic activities, confined to the respective second NRPS enzyme: compared with ViscB, WlpB incorporates D-Leu instead of L-Leu (fifth module) and MassB attaches D-*allo*-Ile instead of D-Val (fourth module). Most remarkably, however, the *wlp*-encoded NRPSs share only about 60–65% amino acid identity with their *wip*-encoded counterparts (Table S1), although both systems synthesize the same lipopeptide. Comparison of the linked genes predicted to encode a LuxR-type regulator (WipR) and a tripartite export system (WipD-WipE-WipF; homologues of MacA, MacB and OprM respectively) reveals the same unexpected trend of much higher similarity between components of the Wip and Visc/Mass systems (producing structural variants) compared with the rather low similarity between those of the Wip and Wlp systems (producing the same secondary metabolite) (Table S1). Comparison of the amino acid identities of the predicted export proteins between the Wip and Wlp systems reveals a higher level of homology than observed for the NRPSs: 67%, 75% and 81% amino acid identity for the outer membrane proteins (WipF/WlpF), periplasmic adaptor proteins (WipD/WlpD) and inner membrane ABC transporters (WipE/WlpE) respectively. This better conservation may be due in part to structural requirements imposed by the assembly of the three export modules in the cell envelope. It is not known whether this type of lipopeptide-associated system, coexpressed with the cognate biosynthetic genes (Lim *et al*., 2009; Rokni-Zadeh *et al*., 2012), may also export other substrates or assist in efflux. Mutational analysis of the export genes downstream of the putisolvin (Dubern *et al*., 2008), arthrofactin (Lim *et al*., 2009) and syringopeptin (Cho and Kang, 2012) biosynthetic operons revealed a strongly reduced but not abolished lipopeptide production, indicating the existence of alternative export routes. For WLIP production by strain RW10S2 a functional linked LuxR-family regulator (WlpR) is essential (Rokni-Zadeh *et al*., 2012), which also applies to its counterparts involved in production of syringofactin (Berti *et al*., 2007), putisolvin (Dubern *et al*., 2008), viscosin (de Bruijn and Raaijmakers, 2009), arthrofactin (Washio *et al*., 2010) and entolysin (Vallet-Gely *et al*., 2010). The low degree of amino acid sequence conservation between the cognate LuxR-family regulators WipR and WlpR (55% identity; Table S1) suggests that some environmental cues controlling WLIP production may differ between the *P. putida* RW10S2 and *P. fluorescens* LMG 5329, possibly reflecting adaptation to the different niches of origin (wetland rice rhizosphere and cultivated mushroom respectively).

Inspection of the genomic DNA regions flanking the *wip* and *visc* clusters revealed a pronounced synteny of highly homologous genes (Fig. 2). This is most prominent for the genes down- and upstream of the *wipBC*/*viscBC* genes. In the latter regions several very similarly organized pyoverdine genes are located (Fig. S1). Homologues of some of these *pvd* genes are equally positioned upstream of the *wlpBC* cluster, but in a different organization and encoding gene products with a significantly lower pairwise amino acid sequence identity (Table S2). Whereas no pyoverdine NRPS is encoded by the *wlpBC*-upstream region, the *wipBC*-upstream region contains three genes for such enzymes (*orf6*, *orf7*, *orf8*) compared with two genes (*pvdI*, *pvdJ*) located upstream of *viscBC*. Orf6 is a homologue of SBW25 PvdI and Orf8 is similar to SBW25 PvdJ, but contains an extra N-terminal module. With involvement of the additional bimodular Orf7, the LMG 5329 pyoverdine would contain a peptidic backbone of 10 amino acids. Elucidation of the SBW25 pyoverdine structure has revealed seven amino acids: D-Ser–L-Lys–Gly–L-foOHOrn–L-Lys–D-foOHOrn–L-Ser (FoOHOrn = *N*5-formyl-*N*5-hydroxyornithine; Moon *et al*., 2008). For strain LMG 5329, the predicted peptide backbone contains three extra amino acids inserted between L-foOHOrn and

© 2012 Society for Applied Microbiology and Blackwell Publishing Ltd, *Environmental Microbiology Reports*

UNCORRECTED PROOF

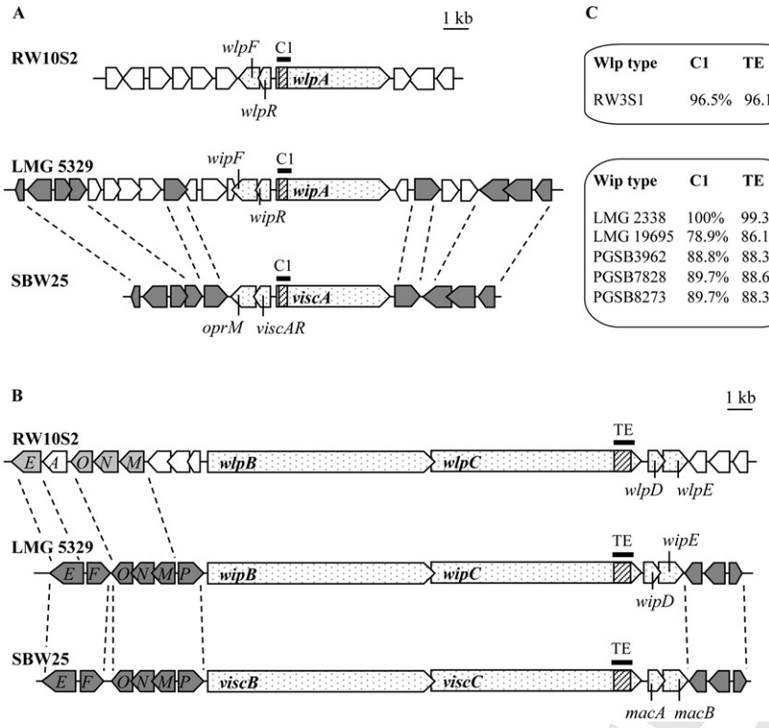

Fig. 2. Genomic context of *wlp*, *wip* and *visc* regions in *P. putida* RW10S2, *P. 'reactans'* LMG 5329 and *P. fluorescens* SBW25 respectively. The two unlinked genomic regions are depicted separately (A with lipoinitiating NRPS; B with middle and terminating NRPSs). Dotted arrows represent the common genes assigned to the WLIP and viscosin systems. Flanking genes are not specified except for the pyoverdine biosynthesis (*pvd*) genes that are labelled with *A*, *E*, *F*, *M*, *N*, *O* and *P*. Organization and functions of the pyoverdine genes are further described in Table S2 and Fig. S1. Pairwise homology among flanking genes between strains is indicated by differential shading of the corresponding arrows: white (unrelated gene products), light grey (~75% amino acid identity) or dark grey (> 90% amino acid identity). Synteny among flanking genes or gene clusters is delineated with dashed lines. Diagonal line-filled boxes correspond to parts of the C1 and TE domains for which PCR amplicons were generated from WLR-positive strains (Rokni-Zadeh *et al.*, 2011). In C, these strains are grouped according to pairwise identity of amplicon-deduced amino acid sequences to either the RW10S2 Wlp proteins (*Pseudomonas* sp. RW3S1) or the LMG 5329 Wip proteins (*P. 'reactans'* LMG 2338, *P. extremorientalis* LMG 19695, *Pseudomonas* spp. PGSB3962, PGSB7828, PGSB8273).

L-Lys (Fig. S1). This matches the peptide chain of *P. fluorescens* strain 18.1 pyoverdine (Kilz *et al.*, 1999). Munsch and colleagues (2000) assigned strain LMG 5329 to siderovar 4 among *P. 'reactans'* isolates. The capability of this siderovar type to incorporate iron mediated by the strain 18.1 pyoverdine supports the proposed LMG 5329 pyoverdine structure.

No synteny is apparent for the *wlpBC*-downstream and *wlpA*-flanking regions with the equivalent *wip/visc* genomic regions. Also in the *viscA* and *wipA* flanking regions many homologues are shared by strains LMG 5329 and SBW25, although in the former several additional interspersed genes are present.

Taxonomic assignment of P. 'reactans' *LMG 5329*

The relatedness among the host strains carrying the *visc*, *wlp* and *wip* genes was further examined by phylogenetic analysis of 20 housekeeping genes (Fig. 3). WLIP producer LMG 5329, isolated from mushroom, grouped tightly with viscosin producer SBW25, representative of subclade 3 within the *P. fluorescens* branch (Loper *et al.*, 2012). Conversely, the other WLIP producer, rice rhizosphere isolate RW10S2, is clearly associated with the *P. putida–Pseudomonas entomophila* cluster. The insect pathogen *P. entomophila* is a close relative of *P. putida* (Silby *et al.*, 2011; Mulet *et al.*, 2012). A similar clustering pattern was observed in the corresponding 16S rRNA phylogenetic tree (Fig. S2; 16S rRNA sequence of LMG 5329 submitted to GenBank under accession number JQ974027). These analyses identify *P. 'reactans'* LMG 5329 as an authentic *P. fluorescens* strain and further substantiate its phylogenetic distance from another WLIP producer, *P. putida* RW10S2, already inferred from comparison of the WLIP gene clusters and their genomic contexts.

Comparative analysis of genetic backbones for WLIP production

A sequence comparison of the entire multi-modular NRPS enzymes does not provide information about the extent of inter-strain similarity for individual modules and for the respective domains within these modules The existence of two apparently divergent biosynthetic systems for the same complex secondary metabolite produced by strains of two different species was therefore further scrutinized by comparative analysis of the NRPS domains [adenylation (A) and condensation (C) domains of each module and the tandem thioesterase (TE) domain]. This analysis, which was extended to the associated regulator and export system, included similarly organized *Pseudomonas* NRPS systems that produce lipopeptides from other groups: arthrofactin (lipoundecapeptide, Roongsawang *et al.*, 2003), syringafactin (lipooctapeptide, Berti *et al.*, 2007), orfamide (lipodecapeptide, Gross *et al.*,

© 2012 Society for Applied Microbiology and Blackwell Publishing Ltd, *Environmental Microbiology Reports*

UNCORRECTED PROOF

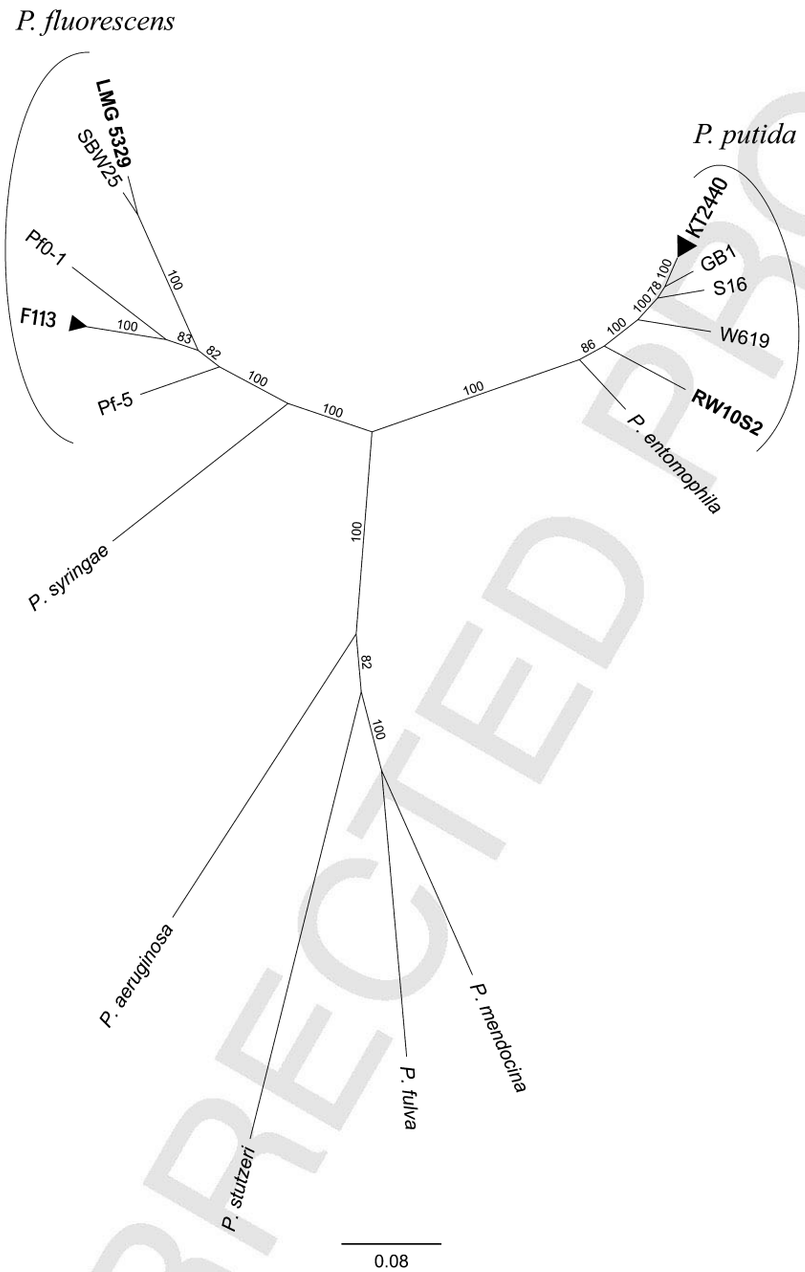

Fig. 3. Phylogenetic relationship of WLIP-producing strains to representative *Pseudomonas* species. From an alignment of 20 concatenated amino acid sequences, representing proteins with diverse housekeeping functions (listed in *Supporting information*), a maximum-likelihood tree using PhyML (JTT matrix; Guindon and Gascuel, 2003), as implemented in Geneious Pro 5.6.3 (Drummond *et al.*, 2011), was constructed for WLIP producers LMG 5329 and RW10S2 (labelled in bold), *Pseudomonas aeruginosa* PAO1, *Pseudomonas brassicacearum* NFM421, *P. entomophila* L48, *P. fluorescens* strains F113, Pf0-1, Pf-5 and SBW25, *Pseudomonas fulva* 12-X, *Pseudomonas mendocina* ymp, *P. putida* strains BIRD1, F1, GB1, KT2440, S16 and W619, *Pseudomonas stutzeri* A1501 and *Pseudomonas syringae* pv. *tomato* DC3000. The filled triangles represent the tightly clustered strains F113-NFM421 and KT2440-BIRD1-F1 respectively. Bootstrap values (%) and substitutions per site (scale bar) are indicated.

2007), putisolvin (lipododecapeptide, Dubern *et al.*, 2008) and entolysin (lipotetradecapeptide, Vallet-Gely *et al.*, 2010).

A coherent picture emerges from the phylotrees of the C-domains (Fig. 4A), as well as of the A-domains (Figs S3 and S4) and the TE domains (Fig. S5): the Wip sequences cluster closely with those of Visc and Mass, but separately from the Wlp sequences that consistently branch off together with those derived from the Pso (putisolvin) and Etl (entolysin) systems. The same observation

© 2012 Society for Applied Microbiology and Blackwell Publishing Ltd, *Environmental Microbiology Reports*

UNCORRECTED PROOF

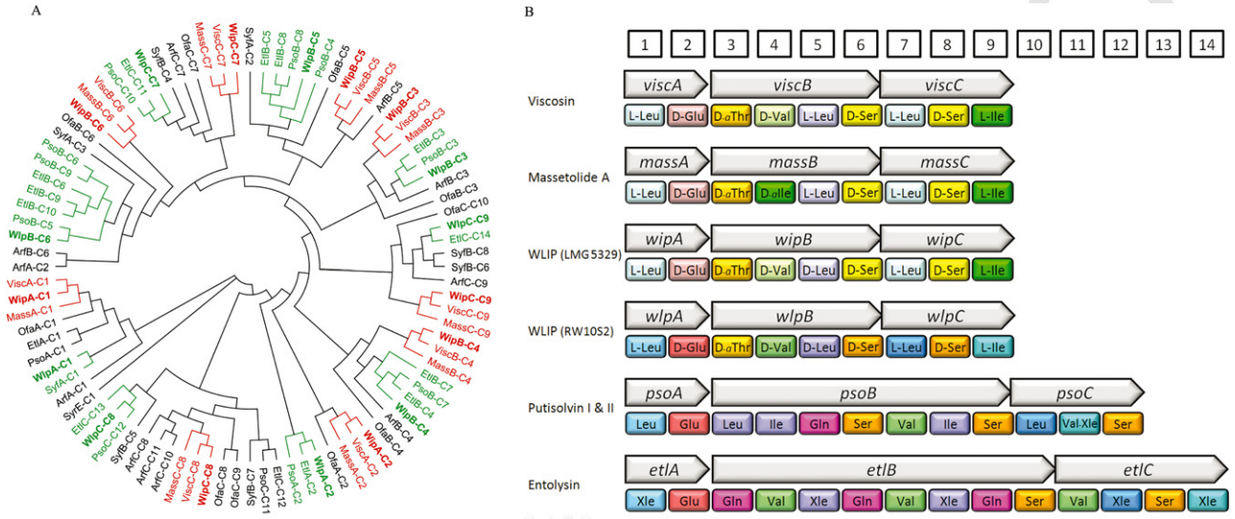

Fig. 4. Comparative analysis of selected domains in the modules of the NRPS enzymes of the Wip and Wlp systems.
A. Cladogram of maximum-likelihood tree inferred from amino acid alignment of C-domains extracted from representative functionally characterized *Pseudomonas* NRPSs. NRPS enzymes are designated with lipopeptide-specific codes: Arf (arthrofactin, *Pseudomonas* sp. MIS38); Etl (entolysin, *P. entomophila* L48); Mass (massetolide, *P. fluorescens* SS101); Ofa (orfamide, *P. fluorescens* Pf-5); Pso (putisolvin, *P. putida* PCL1445); Syf (syringafactin, *P. syringae* DC3000); Visc (viscosin, *P. fluorescens* SBW25); Wip [WLIP, *P. fluorescens* (*P. 'reactans'*) LMG 5329] and Wlp (WLIP, *P. putida* RW10S2). The tree was rooted with the divergent SyrE-C1 domain (syringomycin, *P. syringae* pv. *syringae* strain B301D). Clusters highlighted in red or green colour contain domains derived from Wip (in bold) or Wlp (in bold) respectively. The clustering based on the catalytic type of C-domain (lipoinitiation, non-epimerizing, epimerizing) is indicated in an expanded phylotree (Fig. S7).
B. Similarity of A-domains among *Pseudomonas* strains synthesizing the lipopeptides entolysin, massetolide, putisolvin, viscosin or WLIP. For each lipopeptide, the order of the three enzymes and of the modules therein reflects co-linear incorporation of the amino acid substrates indicated (positions corresponding to numbered boxes). The resulting peptide sequence of only the major massetolide of *P. fluorescens* SS101 is shown (de Bruijn *et al.*, 2008). The respective initiating NRPS genes are located in a genomic region unlinked to the gene pairs encoding the middle and terminating NRPSs, except for the contiguous putisolvin genes (*psoABC*; Dubern *et al.*, 2008). If known, the absolute configuration of the amino acids is indicated. Xle indicates that the residue's identity (either Leu or Ile) was not elucidated (Dubern *et al.*, 2008; Vallet-Gely *et al.*, 2010). Colour coding is based on co-clustering in a maximum-likelihood tree constructed from alignment of A-domain sequences (cladogram shown in Fig. S3). Clades with the same or similar amino acids (hydrophobic residues Ile/Val/Leu; hydroxylated amino acids Ser/Thr) are shown with different shades of a colour (colour assignment based on phylogenetic tree with correspondingly coloured branches shown in Fig. S4).

is made when comparing the associated regulatory and export proteins (Fig. S6). The similarity of the Wlp/Pso/Etl biosynthetic, regulatory and export systems is remarkable as their products differ strongly in peptide sequence and length (Fig. 4B) and, hence, are classified into three different lipopeptide groups (Gross and Loper, 2009).

Balibar and colleagues (2005) showed that the D-configuration of amino acids in arthrofactin is due to the additional epimerization activity of a condensation domain with a distinctive primary sequence, acting on the amino acid attached to the previous module. WLIP differs from viscosin by a different stereochemistry at position 5. Hence, the catalytic activity of the respective C-domains of the following module (C6) is expected to cause this difference. Phylogenetic analysis assigns WipB-C6 and WlpB-C6 to the epimerizing branch among condensation domains, in line with the presence of a D-Leu at the fifth position (Fig. S7). However, ViscB-C6 co-clusters with WipB-C6, thus constituting a notable exception to the Balibar rule, along with the corresponding domains of massetolide (MassB-C6) and orfamide (OfaB-C6) (de Bruijn and Raaijmakers, 2007; 2008; Gross *et al.*, 2007). Amino acid sequence alignment of these domains with the equivalent prototypical arthrofactin ArfB-C6 domain did not reveal a diagnostic sequence or motif potentially linked to the different activities of the viscosin and WLIP biosynthetic enzymes (Fig. S8).

To visualize the phylogenetic relatedness among A-domains, a colour code was assigned to the different branches in the corresponding phylotree (Fig. S4), based on patristic distances as a measure of evolutionary divergence (Table S3). This differentiation among A-domains was applied to both WLIP biosynthetic systems in comparison with related *Pseudomonas* lipopeptide NRPSs (Fig. 4B). This representation clearly highlights the dual nature of WLIP production by the Wip and Wlp systems: the Wlp-type WLIP system is related to those of entolysin (Etl) and putisolvin (Pso) in the *P. putida–P. entomophila*

© 2012 Society for Applied Microbiology and Blackwell Publishing Ltd, *Environmental Microbiology Reports*

UNCORRECTED PROOF

group, while the Wip-type WLIP system is more similar to the massetolide (Mass) and Visc (viscosin) ones of the *P. fluorescens* group.

WLIP biosynthesis: same product but distinct genes in different hosts

Previously, a PCR-based screening for lipopeptide-specific NRPS genes in *Pseudomonas* based on amplification and sequencing of part of the unique C1 and TE domains also yielded amplicons for a number of WLR-positive *Pseudomonas* strains from different origins (Rokni-Zadeh *et al*., 2011). In retrospect, among these isolates no additional or intermediate genotypes with respect to WLIP genes appear to be present as the diagnostic amplicon sequences (corresponding to stretches for the lipoinitiation domain and the terminal tandem thioesterase domain as indicated in Fig. 2) can be assigned to either the Wlp type (rice rhizosphere isolate RW3S1 from Sri Lanka) or to the Wip type (five strains). The latter type was identified for a mushroom isolate from the UK (LMG 2338), for three strains originating from the rhizosphere of maize in Belgium (PGSB3962, PGSB7828, PGSB8273), and for *Pseudomonas extremorientalis* LMG 19695, a strain affiliated with the *P. fluorescens* cluster that was isolated from a drinking water reservoir in Russia (Ivanova *et al*., 2002).

From an evolutionary viewpoint, the occurrence of two distinct NRPS systems generating the same secondary metabolite conferring similar phenotypes upon phylogenetically distinct hosts is of particular interest. The high similarity of the Wip and Visc genes and close relatedness of their respective representative hosts (*P. fluorescens* LMG 5329 and SBW25) suggests that these lipopeptide systems diverged relatively recently to produce two lipopeptides that merely differ by the D/L-configuration of one amino acid residue. Apparently, WLIP biosynthesis has evolved independently in another host of the *P. putida* clade. This is inferred from homology of the Wlp components with NRPS systems assembling the structurally unrelated lipopeptides putisolvin and entolysin, and from common affiliation of their host strains with the *P. putida*–*P. entomophila* clade. Analysis of the Wlp/Pso/Etl substrate-selecting domains (Fig. 4B) reveals a prominent example of patchwork assembly of similar NRPS modules recruited to generate lipopeptides of different amino acid sequences and lengths.

The identification of WLIP genes in strains of *P. fluorescens* and *P. putida*, both behaving as *P. 'reactans'*, clearly urges the discontinuation of the use of this invalid species designation, originally based on a diagnostic phenotype linked to secondary metabolism, which is still propagating in research papers and reviews (Kobayashi and Crouch, 2009; Park *et al*., 2009; Largeteau and Savoie, 2010; Oksinska *et al*., 2011; Prashanth *et al*., 2011; Shirokova *et al*., 2012).

Acknowledgements

The authors acknowledge assistance of G. Schoofs (CMPG, KU Leuven) with Tn*5* mutagenesis and of D. De Coster (CMPG, KU Leuven) with Southern blot analysis. This work was supported by a KU Leuven–Zhejiang University SBA fellowship to W. L. and grant GOA/011/2008 (KU Leuven Research Council). E. Y. was supported by a Flemish Interuniversity Council (Vlaamse Interuniversitaire Raad/VLIR) scholarship.

References

Aziz, R.K., Bartels, D., Best, A.A., DeJongh, M., Disz, T., Edwards, R.A., *et al*. (2008) The RAST Server: rapid annotations using subsystems technology. *BMC Genomics* **9:** 75.

Balibar, C.J., Vaillancourt, F.H., and Walsh, C.T. (2005) Generation of D amino acid residues in assembly of arthrofactin by dual condensation/epimerization domains. *Chem Biol* **12:** 1189–1200.

Berti, A.D., Greve, N.J., Christensen, Q.H., and Thomas, M.G. (2007) Identification of a biosynthetic gene cluster and the six associated lipopeptides involved in swarming motility of *Pseudomonas syringae* pv. *tomato* DC3000. *J Bacteriol* **189:** 6312–6323.

Boulnois, G.J., Varley, J.M., Sharpe, G.S., and Franklin, F.C. (1985) Transposon donor plasmids, based on ColIb-P9, for use in *Pseudomonas putida* and a variety of other Gram negative bacteria. *Mol Gen Genet* **200:** 65–67.

de Bruijn, I., and Raaijmakers, J.M. (2009) Diversity and functional analysis of LuxR-type transcriptional regulators in cyclic lipopeptide biosynthesis in *Pseudomonas fluorescens*. *Appl Environ Microbiol* **75:** 4753–4761.

de Bruijn, I., de Kock, M.J., Yang, M., de Waard, P., van Beek, T.A., and Raaijmakers, J.M. (2007) Genome-based discovery, structure prediction and functional analysis of cyclic lipopeptide antibiotics in *Pseudomonas* species. *Mol Microbiol* **63:** 417–428.

de Bruijn, I., de Kock, M.J., de Waard, P., van Beek, T.A., and Raaijmakers, J.M. (2008) Massetolide A biosynthesis in *Pseudomonas fluorescens*. *J Bacteriol* **190:** 2777–2789.

Cho, H., and Kang, H. (2012) The PseEF efflux system is a virulence factor of *Pseudomonas syringae* pv. *syringae*. *J Microbiol* **50:** 79–90.

Drummond, A., Ashton, B., Cheung, M., Heled, J., Kearse, M., Moir, R., *et al*. (2011) *Geneious v5.6.3*. URL http://www.geneious.com/

Dubern, J.F., Coppoolse, E.R., Stiekema, W.J., and Bloemberg, G.V. (2008) Genetic and functional characterization of the gene cluster directing the biosynthesis of putisolvin I and II in *Pseudomonas putida* strain PCL1445. *Microbiology* **154:** 2070–2083.

Gross, H., and Loper, J.E. (2009) Genomics of secondary metabolite production by *Pseudomonas* spp. *Nat Prod Rep* **26:** 1408–1446.

Gross, H., Stockwell, V.O., Henkels, M.D., Nowak-

© 2012 Society for Applied Microbiology and Blackwell Publishing Ltd,

UNCORRECTED PROOF

Thompson, B., Loper, J.E., and Gerwick, W.H. (2007) The genomisotopic approach: a systematic method to isolate products of orphan biosynthetic gene clusters. *Chem Biol* **14:** 53–63.

Guindon, S., and Gascuel, O. (2003) A simple, fast, and accurate algorithm to estimate large phylogenies by maximum likelihood. *Syst Biol* **52:** 696–704.

Ishikawa, J., and Hotta, K. (1999) FramePlot: a new implementation of the Frame analysis for predicting protein-coding regions in bacterial DNA with a high G+C content. *FEMS Microbiol Lett* **174:** 251–253.

Ivanova, E.P., Gorshkova, N.M., Sawabe, T., Hayashi, K., Kalinovskaya, N.I., Lysenko, A.M., *et al.* (2002) *Pseudomonas extremorientalis* sp. nov., isolated from a drinking water reservoir. *Int J Syst Evol Microbiol* **52:** 2113–2120.

Kilz, S., Lenz, C., Fuchs, R., and Budzikiewicz, H. (1999) A fast screening method for the identification of siderophores from fluorescent *Pseudomonas* spp. by liquid chromatography/electrospray mass spectrometry. *J Mass Spectrom* **34:** 281–290.

Kobayashi, D.Y., and Crouch, J.A. (2009) Bacterial/fungal interactions: from pathogens to mutualistic endosymbionts. *Annu Rev Phytopathol* **47:** 63–82.

Largeteau, M.L., and Savoie, J.M. (2010) Microbially induced diseases of *Agaricus bisporus*: biochemical mechanisms and impact on commercial mushroom production. *Appl Microbiol Biotechnol* **86:** 63–73.

Lim, S.P., Roongsawang, N., Washio, K., and Morikawa, M. (2009) Flexible exportation mechanisms of arthrofactin in *Pseudomonas* sp. MIS38. *J Appl Microbiol* **107:** 157–166.

Lo Cantore, P., Lazzaroni, S., Coraiola, M., Serra, M.D., Cafarchia, C., Evidente, A., and Lacobellis, N.S. (2006) Biological characterization of white line-inducing principle (WLIP) produced by *Pseudomonas reactans* NCPPB1311. *Mol Plant Microbe Interact* **19:** 1113–1120.

Loper, J.E., Hassan, K.A., Mavrodi, D.V., Davis, E.W., II, Lim, C.K., Shaffer, B.T., *et al.* (2012) Comparative genomics of plant-associated *Pseudomonas* spp.: insights into diversity and inheritance of traits involved in multitrophic interactions. *PLoS Genet* **8:** e1002784.

Martin, V.J., and Mohn, W.W. (2002) The isolation of DNA sequences flanking Tn*5* transposon insertions by inverse PCR. *Methods Mol Biol* **192:** 315–323.

Moon, C.D., Zhang, X.X., Matthijs, S., Schäfer, M., Budzikiewicz, H., and Rainey, P.B. (2008) Genomic, genetic and structural analysis of pyoverdine-mediated iron acquisition in the plant growth-promoting bacterium *Pseudomonas fluorescens* SBW25. *BMC Microbiol* **8:** 7.

Mulet, M., Gomila, M., Lemaitre, B., Lalucat, J., and Garcia-Valdes, E. (2012) Taxonomic characterisation of *Pseudomonas* strain L48 and formal proposal of *Pseudomonas entomophila* sp. nov. *Syst Appl Microbiol* **35:** 145–149.

Munsch, P., and Alatossava, T. (2002) The white-line-in-agar test is not specific for the two cultivated mushroom associated pseudomonads, *Pseudomonas tolaasii* and *Pseudomonas 'reactans'*. *Microbiol Res* **157:** 7–11.

Munsch, P., Geoffroy, V.A., Alatossava, T., and Meyer, J.M. (2000) Application of siderotyping for characterization of *Pseudomonas tolaasii* and *'Pseudomonas reactans'* isolates associated with brown blotch disease of cultivated mushrooms. *Appl Environ Microbiol* **66:** 4834–4841.

Oksinska, M.P., Wright, S.A.I., and Pietr, S.J. (2011) Colonization of wheat seedlings (*Triticum aestivum* L.) by strains of *Pseudomonas* spp. with respect to their nutrient utilization profiles. *Eur J Soil Biol* **47:** 364–373.

Park, S.H., Lim, J.A., Choi, J.S., Kim, K.A., and Joo, C.K. (2009) The resistance patterns of normal ocular bacterial flora to 4 fluoroquinolone antibiotics. *Cornea* **28:** 68–72.

Prashanth, S.N., Bianco, G., Cataldi, T.R., and Iacobellis, N.S. (2011) Acylhomoserine lactone production by bacteria associated with cultivated mushrooms. *J Agric Food Chem* **59:** 11461–11472.

Raaijmakers, J.M., de Bruijn, I., and de Kock, M.J. (2006) Cyclic lipopeptide production by plant-associated *Pseudomonas* spp.: diversity, activity, biosynthesis, and regulation. *Mol Plant Microbe Interact* **19:** 699–710.

Raaijmakers, J.M., De Bruijn, I., Nybroe, O., and Ongena, M. (2010) Natural functions of lipopeptides from *Bacillus* and *Pseudomonas*: more than surfactants and antibiotics. *FEMS Microbiol Rev* **34:** 1037–1062.

Rokni-Zadeh, H., Mangas-Losada, A., and De Mot, R. (2011) PCR detection of novel non-ribosomal peptide synthetase genes in lipopeptide-producing *Pseudomonas*. *Microb Ecol* **62:** 941–947.

Rokni-Zadeh, H., Li, W., Sanchez-Rodriguez, A., Sinnaeve, D., Rozenski, J., Martins, J.C., and De Mot, R. (2012) Genetic and functional characterization of cyclic lipopeptide WLIP production by rice rhizosphere isolate *Pseudomonas putida* RW10S2. *Appl Environ Microbiol* **78:** 4826–4834.

Roongsawang, N., Hase, K., Haruki, M., Imanaka, T., Morikawa, M., and Kanaya, S. (2003) Cloning and characterization of the gene cluster encoding arthrofactin synthetase from *Pseudomonas* sp. MIS38. *Chem Biol* **10:** 869–880.

Roongsawang, N., Washio, K., and Morikawa, M. (2011) Diversity of nonribosomal peptide synthetases involved in the biosynthesis of lipopeptide biosurfactants. *Int J Mol Sci* **12:** 141–172.

Röttig, M., Medema, M.H., Blin, K., Weber, T., Rausch, C., and Kohlbacher, O. (2011) NRPSpredictor2-a web server for predicting NRPS adenylation domain specificity. *Nucleic Acids Res* **39:** W362–W367.

Sajben, E., Manczinger, L., Nagy, A., Kredics, L., and Vagvolgyi, C. (2011) Characterization of pseudomonads isolated from decaying sporocarps of oyster mushroom. *Microbiol Res* **166:** 255–267.

Shirokova, L.S., Benezeth, P., Pokrovsky, O.S., Gerard, E., Menez, B., and Alfredsson, H. (2012) Effect of the heterotrophic bacterium *Pseudomonas reactans* on olivine dissolution kinetics and implications for CO_2 storage in basalts. *Geochim Cosmochim Acta* **80:** 30–50.

Silby, M.W., Cerdeño-Tárraga, A.M., Vernikos, G.S., Giddens, S.R., Jackson, R.W., Preston, G.M., *et al.* (2009) Genomic and genetic analyses of diversity and plant interactions of *Pseudomonas fluorescens*. *Genome Biol* **10:** R51.

Silby, M.W., Winstanley, C., Godfrey, S.A., Levy, S.B., and Jackson, R.W. (2011) *Pseudomonas* genomes: diverse and adaptable. *FEMS Microbiol Rev* **35:** 652–680.

Vallet-Gely, I., Novikov, A., Augusto, L., Liehl, P., Bolbach, G., Pechy-Tarr, M., *et al.* (2010) Association of hemolytic activity of *Pseudomonas entomophila*, a versatile soil bacte-

UNCORRECTED PROOF

rium, with cyclic lipopeptide production. *Appl Environ Microbiol* **76:** 910–921.

Washio, K., Lim, S.P., Roongsawang, N., and Morikawa, M. (2010) Identification and characterization of the genes responsible for the production of the cyclic lipopeptide arthrofactin by *Pseudomonas* sp. MIS38. *Biosci Biotechnol Biochem* **74:** 992–999.

Wong, W.C., and Preece, T.F. (1979) Identification of *Pseudomonas tolaasii*: the white line in agar and mushroom tissue block rapid pitting tests. *J Appl Bacteriol* **47:** 401–407.

Wu, X., Monchy, S., Taghavi, S., Zhu, W., Ramos, J., and van der Lelie, D. (2011) Comparative genomics and functional analysis of niche-specific adaptation in *Pseudomonas putida*. *FEMS Microbiol Rev* **35:** 299–323.

Zerbino, D.R., and Birney, E. (2008) Velvet: algorithms for de novo short read assembly using de Bruijn graphs. *Genome Res* **18:** 821–829.

Supporting information

Additional Supporting Information may be found in the online version of this article:

Fig. S1. Organization of the pyoverdine genes located upstream of the second lipopeptide biosynthetic gene cluster in *P. putida* RW10S2, *P. 'reactans'* LMG 5329 and *P. fluorescens* SBW25. For the encoded NRPS enzymes the predicted domains (labelled circles) are indicated: C, condensation; A, adenylation; T, thiolation; E, epimerization; TE, thioesterase. For *P. fluorescens* SBW25 the peptide chain that is synthesized by PvdI and PvdJ is indicated (Moon *et al*., 2008, *BMC Microbiol* **8:** 7). Amino acids are identified by the standard three-letter code (FoOHOrn = *N*5-formyl-*N*5-hydroxyornithine). The amino acid specificity of the modules inferred from A-domain analysis (NRPSpredictor2; Röttig *et al*., 2011, *Nucleic Acids Res* **39:** W362–W367) is shown for the putative pyoverdine synthetases (Orf6, Orf7, Orf8) of strain LMG 5329. Three amino acids predicted for the LMG 5329 pyoverdine that are absent in the SBW25 pyoverdine are shown in dashed boxes. No other pyoverdine genes are located downstream of *fpvA* in strain RW10S2.

Fig. S2. 16S rRNA phylogenetic relationship of WLIP-producing strains RW10S2 and LMG 5329 to representative *Pseudomonas* species. The bacterial labels are as indicated in Fig. 3. *E. coli* K-12 substr. MG1655 16S rRNA was used an out-group. Bootstrap values (%) and substitutions per site (scale bar) are indicated.

Fig. S3. Cladogram of maximum-likelihood tree inferred from amino acid alignment of A-domains extracted from representative functionally characterized *Pseudomonas* NRPSs. NRPS enzymes are designated with lipopeptide-specific codes: Arf (arthrofactin, *Pseudomonas* sp. MIS38); Etl (entolysin, *P. entomophila* L48); Mass (massetolide, *P. fluorescens* SS101); Ofa (orfamide, *P. fluorescens* Pf-5); Pso (putisolvin, *P. putida* PCL1445); Syf (syringafactin, *P. syringae* DC3000); Visc (viscosin, *P. fluorescens* SBW25); Wip (WLIP, *P. 'reactans'* LMG 5329) and Wlp (WLIP, *P. putida* RW10S2). For each domain the substrate specificity is indicated in parentheses using the standard three-letter code. The tree was rooted with the divergent SyrB1 domain (syringomycin, *P. syringae* pv. *syringae* strain B301D). Clusters highlighted in red or green colour contain domains derived from Wip (in bold) or Wlp (in bold) respectively.

Fig. S4. Phylogenetic tree of Mass/Visc/Wip/Wlp A-domains corresponding to cladogram representation of Fig. S3. NRPS designation as in Fig. S3. The corresponding matrix with pairwise patristic distance values (Table S3) was used to obtain the differential colour coding for the branches. As an indicator of evolutionary distance, two domains with a patristic distance (summed branches lengths) above 0.45 are represented in a different colour.

Fig. S5. Unrooted maximum-likelihood tree constructed from alignment of TE domains extracted from representative functionally characterized *Pseudomonas* NRPSs. NRPS designation as in Fig. S3. Clusters highlighted in red or green colour encompass domains derived from Wip (in bold) or Wlp (in bold) respectively. Bootstrap values (%) and substitutions per site (scale bar) are indicated.

Fig. S6. Phylogenetic analysis of proteins associated with representative functionally characterized *Pseudomonas* NRPS systems: LuxR-type regulators (A) and homologues of MacA (B), MacB (C) and OprM (D). NRPS designation as in Fig. S3. The OprM equivalents of the Syf and Arf systems are not yet known. Clusters highlighted in red or green colour encompass domains derived from Wip (in bold) or Wlp (in bold) respectively. Bootstrap values (%) and substitutions per site (scale bar) are indicated.

Fig. S7. Maximum-likelihood tree inferred from alignment of C-domains extracted from representative functionally characterized *Pseudomonas* NRPSs. NRPS enzymes are designated with lipopeptide-specific codes: Arf (arthrofactin, *Pseudomonas* sp. MIS38); Etl (entolysin, *P. entomophila* L48); Mass (massetolide, *P. fluorescens* SS101); Ofa (orfamide, *P. fluorescens* Pf-5); Pso (putisolvin, *P. putida* PCL1445); Syf (syringafactin, *P. syringae* pv. *tomato* DC3000); Syp (syringopeptin, *P. syringae* pv. *syringae* B301D); Syr (*P. syringae* pv. *syringae* strain B301D); Visc (viscosin, *P. fluorescens* SBW25); Wip [WLIP, *P. fluorescens* (*P. 'reactans'*) LMG 5329; in red] and Wlp (WLIP, *P. putida* RW10S2; in green). The tree was rooted with the divergent SyrE-C1 domain. The clusters corresponding to lipoinitiation domains (C1), conventional condensation domains (C) and dual condensation/epimerization domains (C/E) are labelled. C-domains deviating from the 'Balibar rule' with respect to the stereochemistry of the amino acid incorporated by the previous module (Balibar *et al*., 2005, *Chem Biol* **12:** 1189–1200) are indicated with {L} in the C/E cluster and with {D} in the C cluster. Sequences used for alignment in Fig. S8 are marked in bold.

Fig. S8. Multiple amino acid sequence alignment of the C-domains extracted from the sixth module of the NRPSs synthesizing arthrofactin (ArfB), massetolide (MassB), orfamide (OfaB), viscosin (ViscB) and WLIP (WipB, WlpB). The stereochemistry (D or L) of the fifth amino acid present in the respective lipopeptide products is indicated. The positions of a histidine and aspartate residue (red) required for catalytic activity (Bergendahl *et al*., 2002, *Eur J Biochem* **269:** 620–629) and the additional N-terminal extended His-motif (H-H-I/L-X_4-G-D; blue) identified by Balibar and colleagues (2005, *Chem Biol* **12:** 1189–1200) in C/E-type domains are marked.

© 2012 Society for Applied Microbiology and Blackwell Publishing Ltd, *Environmental Microbiology Reports*

UNCORRECTED PROOF

Table S1. Pairwise amino acid sequence identities of the NRPS enzymes and auxiliary proteins (LuxR-type regulator, homologues of MacA, MacB and OprM) encoded by the gene clusters *mass* (massetolide), *visc* (viscosin), *wlp* (WLIP, strain RW10S2) and *wip* (WLIP, strain LMG 5329).

Table S2. Homology of the pyoverdine genes located upstream of the second lipopeptide biosynthetic gene cluster in *P. putida* RW10S2, *P. 'reactans'* LMG 5329 and *P. fluorescens* SBW25. The respective gene organizations are shown in Fig. S1.

Table S3. Patristic distance matrix for the maximum-likelihood tree of selected *Pseudomonas* NRPS A-domains. The corresponding tree is shown in Fig. S3.

UNCORRECTED PROOF

© 2012 Society for Applied Microbiology and Blackwell Publishing Ltd, *Environmental Microbiology Reports*

AUTHOR QUERY FORM

Dear Author,
During the preparation of your manuscript for publication, the questions listed below have arisen. Please attend to these matters and return this form with your proof.
Many thanks for your assistance.

Query References	Query	Remarks
1	AUTHOR: de Bruijn and Raaijmakers, 2007 and 2008 have not been included in the Reference List; please supply full publication details.	
2	AUTHOR: Please check this website address and confirm that it is correct. (Please note that it is the responsibility of the author(s) to ensure that all URLs given in this article are correct and useable.)	

UNCORRECTED PROOF

WILEY-BLACKWELL

USING e-ANNOTATION TOOLS FOR ELECTRONIC PROOF CORRECTION

Required software to e-Annotate PDFs: Adobe Acrobat Professional or Adobe Reader (version 8.0 or above). (Note that this document uses screenshots from Adobe Reader X)
The latest version of Acrobat Reader can be downloaded for free at: http://get.adobe.com/reader/

Once you have Acrobat Reader open on your computer, click on the Comment tab at the right of the toolbar:

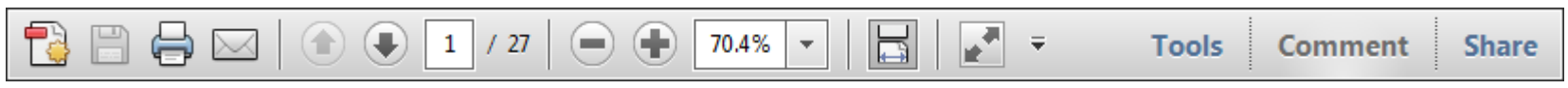

This will open up a panel down the right side of the document. The majority of tools you will use for annotating your proof will be in the Annotations section, pictured opposite. We've picked out some of these tools below:

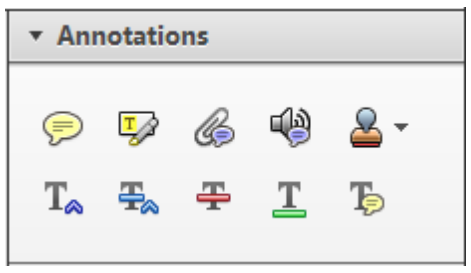

1. Replace (Ins) Tool – for replacing text.

Strikes a line through text and opens up a text box where replacement text can be entered.

How to use it

- Highlight a word or sentence.
- Click on the Replace (Ins) icon in the Annotations section.
- Type the replacement text into the blue box that appears.

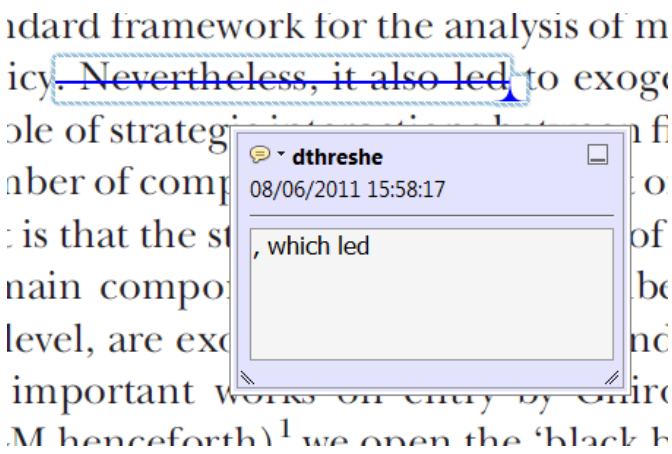

2. Strikethrough (Del) Tool – for deleting text.

Strikes a red line through text that is to be deleted.

How to use it

- Highlight a word or sentence.
- Click on the Strikethrough (Del) icon in the Annotations section.

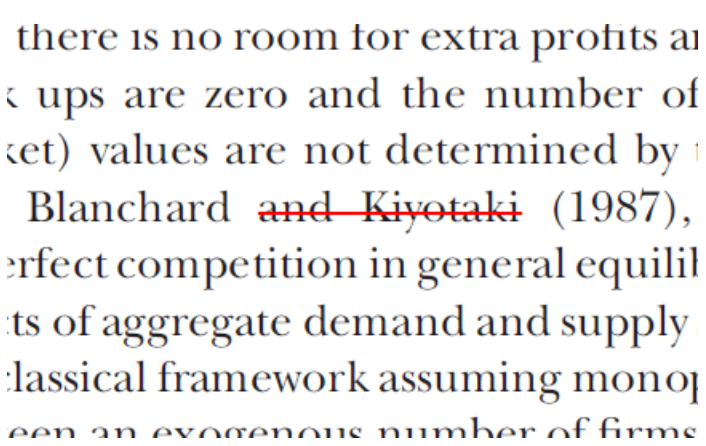

3. Add note to text Tool – for highlighting a section to be changed to bold or italic.

Highlights text in yellow and opens up a text box where comments can be entered.

How to use it

- Highlight the relevant section of text.
- Click on the Add note to text icon in the Annotations section.
- Type instruction on what should be changed regarding the text into the yellow box that appears.

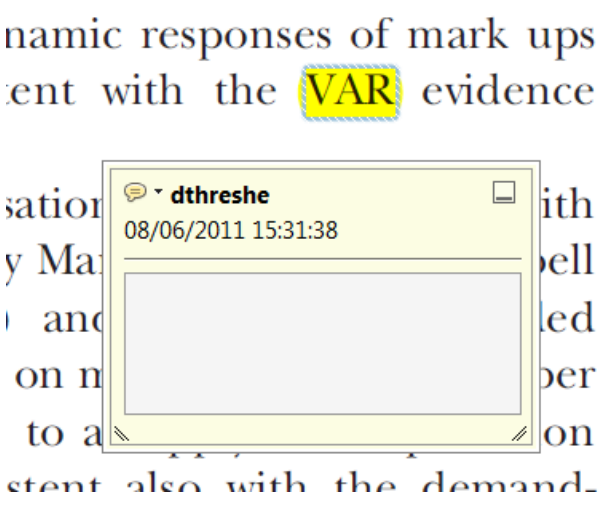

4. Add sticky note Tool – for making notes at specific points in the text.

Marks a point in the proof where a comment needs to be highlighted.

How to use it

- Click on the Add sticky note icon in the Annotations section.
- Click at the point in the proof where the comment should be inserted.
- Type the comment into the yellow box that appears.

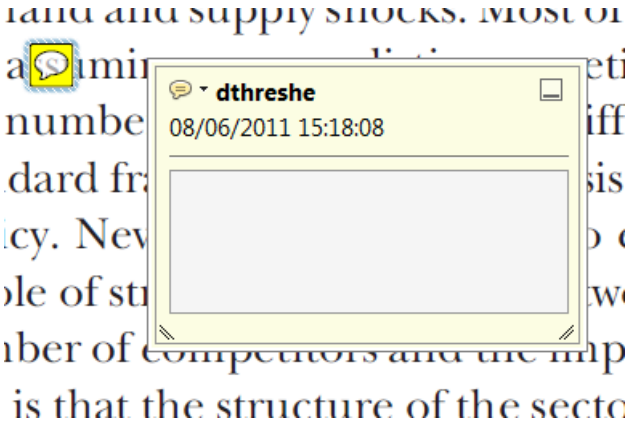

WILEY-BLACKWELL

USING e-ANNOTATION TOOLS FOR ELECTRONIC PROOF CORRECTION

5. Attach File Tool – for inserting large amounts of text or replacement figures.

Inserts an icon linking to the attached file in the appropriate pace in the text.

How to use it

- Click on the Attach File icon in the Annotations section.
- Click on the proof to where you'd like the attached file to be linked.
- Select the file to be attached from your computer or network.
- Select the colour and type of icon that will appear in the proof. Click OK.

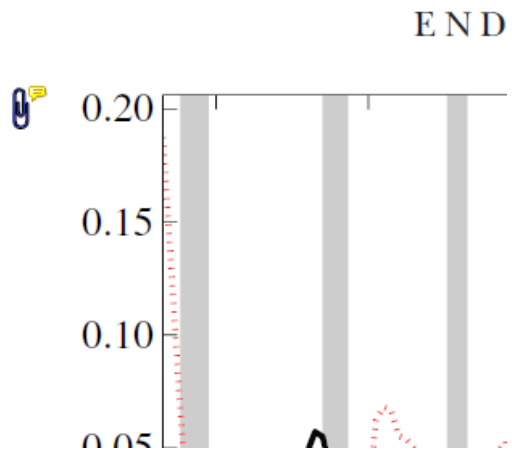

6. Add stamp Tool – for approving a proof if no corrections are required.

Inserts a selected stamp onto an appropriate place in the proof.

How to use it

- Click on the Add stamp icon in the Annotations section.
- Select the stamp you want to use. (The Approved stamp is usually available directly in the menu that appears).
- Click on the proof where you'd like the stamp to appear. (Where a proof is to be approved as it is, this would normally be on the first page).

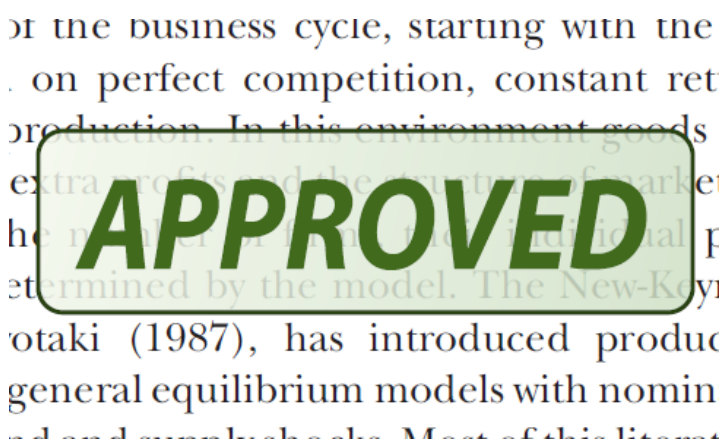

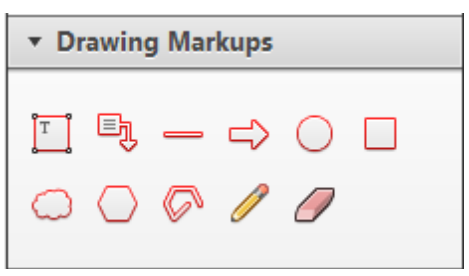

7. Drawing Markups Tools – for drawing shapes, lines and freeform annotations on proofs and commenting on these marks.

Allows shapes, lines and freeform annotations to be drawn on proofs and for comment to be made on these marks..

How to use it

- Click on one of the shapes in the Drawing Markups section.
- Click on the proof at the relevant point and draw the selected shape with the cursor.
- To add a comment to the drawn shape, move the cursor over the shape until an arrowhead appears.
- Double click on the shape and type any text in the red box that appears.

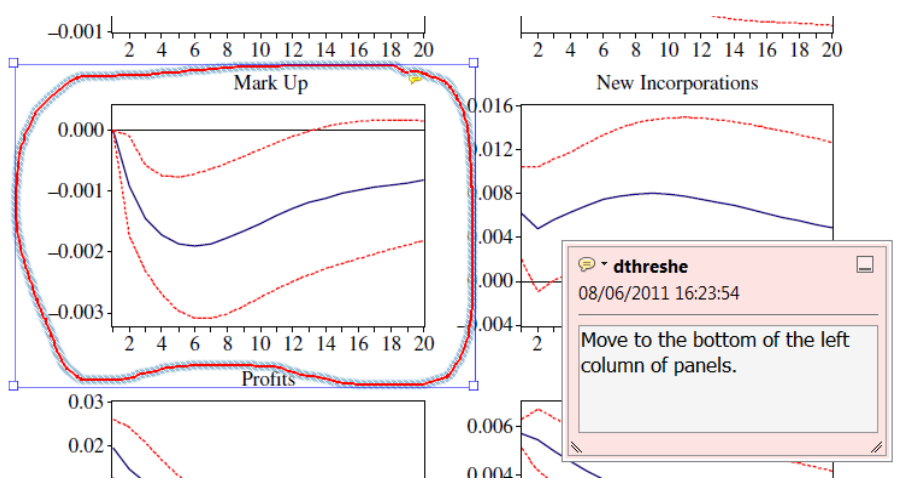

For further information on how to annotate proofs, click on the Help menu to reveal a list of further options: